The American Association of Petroleum Geologists Bulletin
V. 65, No. 12 (December 1981), P. 2506-2520, 16 Figs.

Thrust Loads and Foreland Basin Evolution, Cretaceous, Western United States[1]

TERESA E. JORDAN[2]

ABSTRACT

Two-dimensional modeling of loading during the formation of the Idaho-Wyoming thrust belt shows that regional isostatic compensation by flexure of an elastic lithosphere is sufficient to control the formation of a foreland basin. The flexural rigidity of the lithosphere is inferred to have been approximately 10^{23} Nm (10^{30} dyne cm), on the basis of palinspastic comparison of predicted downwarping, due to the thrust plate loads, to the shape of the sedimentary wedge on the west side of the Cretaceous Western Interior seaway. Erosion of part of the uplifted thrust plates redistributed the load, depositing it farther to the east, thereby causing subsidence over a much wider area than could have been accomplished only by the loading by thrust plates.

Paleotopography after major Cretaceous thrust events was calculated. The resulting mountainous terrain, gentle alluvial plain, and flat sea floor correspond well with the topography of the modern foreland thrust belt and basin system in the Andes of South America and to paleogeographic reconstructions in the western United States thrust belt. Topography is controlled by the subsurface geometry of the thrust faults, particularly the positions of ramp zones, and by isostatic subsidence.

INTRODUCTION

Foreland basins, elongate subsiding troughs flanking the cratonic side of foreland thrust belts, are a characteristic companion of mountain belts throughout the world. Important petroleum reserves exist in strata deposited in those foreland basins. Furthermore, foreland basin sediments record the history of uplift and erosion, and hence deformation, of the adjacent mountain range.

The Idaho-Wyoming salient of the Sevier orogenic belt and the Cretaceous foreland basin on its eastern side are the best understood thrust belt and foreland basin pair in the world. This study quantitatively examines the relations between the evolving orogenic belt and subsiding basin by determining the actual lithospheric load and subsidence through time. Over a span of 70 million years, the major aspects of the basin's subsidence can be accounted for by elastic bending due to regional isostatic compensation of the load added by thrusting and redistributed by erosion and sedimentation.

Two end-member types of foreland basins are in distinctly different tectonic settings (Dickinson, 1974). Retroarc basins form on the cratonic side of foreland thrust belts that are adjacent to magmatic arcs, such as the sedimentary basin forming on the east side of the Subandean thrust belt of the Andes. Peripheral basins form beside foreland thrust belts that are adjacent to suture zones, such as the modern Indo-Gangetic basin south of the Himalayas. Retroarc basins develop during normal subduction of oceanic crust beneath a continent, whereas peripheral basins form during continental collision. Foreland basins may also form in a wide variety of intermediate tectonic settings. The analysis and discussion which follow are specifically derived for a retroarc basin; additional work will be needed to determine which of the following characteristics are also true of peripheral basins.

Tectonic thickening of the crust in the thrust belt has often been cited as a probable driving mechanism for downwarping in the foreland basin (Price, 1973; Dickinson, 1974; Kauffman, 1977). However, only recently has any attempt been made to confirm the role of loading or to determine whether other factors contribute, such as thermally induced subsidence or crustal buckling (Elliott, 1977; Beaumont, 1979, 1981; Lorenz, 1980; Speed and Sleep, 1980).

Recently, significant progress has been made in determining the nature of and mechanisms responsible for various types of sedimentary basins (Sleep and Snell, 1976; Steckler and Watts, 1978; review by Bott, 1979). Beaumont (1979, 1981) modeled subsidence due to loading based on present distribution of foreland basin strata in the Canadian Rockies and Alberta foreland basin. However, few details are known of the time of faulting in the Canadian Rockies, and younger tectonic activity may control present rock distribution. Therefore, his model must solve simultaneously for the load history and for the mechanical response of the crust. While Beaumont's conclusion that the foreland

[1]Manuscript received, January 20, 1981; accepted, July 30, 1981.
[2]Department of Geological Sciences, Cornell University, Ithaca, New York 14853.

This project has been supported by the Cornell Program for Study of the Continents (COPSTOC). F. Royse reviewed an early version of the manuscript and, with R. W. Allmendinger, provided extensive help in understanding age and tectonic relations. D. Elliott reviewed the manuscript. C. Beaumont, C. Angevine, and D. L. Turcotte encouraged the study and aided in developing the mechanical model. I also benefited from discussions with G. Bond, A. Watts, and M. Stecklar. T. Szebenyi's assistance in computer modeling is gratefully appreciated. G. Todd, T. A. Brewer, E. Story, and K. Knowlton prepared the manuscript and illustrations. Cornell Contribution Number 689.

basin subsides by flexure of a viscoelastic plate under a load is significant, greater control on the time of faulting and contributions of other tectonic elements are needed to test the model. The present study of a foreland thrust belt and basin contrasts with the work of Beaumont (1979, 1981) in two significant ways. First, the geologic constraints on the Idaho-Wyoming thrust belt and basin are better known and, second, no assumptions are made about the behavior of the region since the end of the Cretaceous.

IDAHO-WYOMING THRUST BELT AND FORELAND BASIN

Thrust Belt

The Idaho-Wyoming thrust belt (Fig. 1) is a region of thin-skinned thrusting along gently west-dipping sledrunner faults (Fig. 2). Thrusting occurred from the latest Jurassic to the early Eocene, and the ages of thrust faults decrease to the east (Armstrong and Oriel, 1965; Oriel and Armstrong, 1966). In the eastern part, the thrust belt has been shortened by a minimum of 50%, without metamorphism, involvement of crystalline basement, or development of mylonite zones (Royse et al, 1975). Duplication of stratigraphic section accommodated shortening. Existing information on the structural geometry of the thrust belt was compiled by Royse et al (1975) in the form of two east-west cross sections spanning the belt; the northern section (XX′) forms the basis for the analysis of load which follows.

Foreland Basin

The foreland basin of Idaho-Wyoming-Utah forms the western part of the vast Cretaceous Western Interior basin, or seaway, which extended from northern Canada to the Gulf of Mexico and locally was over 1,600 km wide from east to west (Kauffman, 1977).

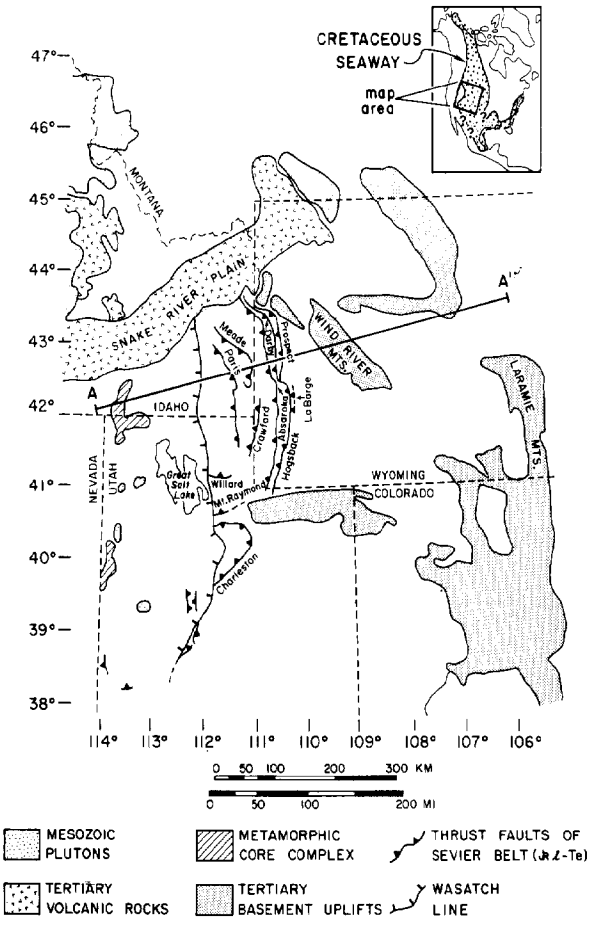

FIG. 1—Location and tectonic map showing relation of Idaho-Wyoming thrust belt to Cretaceous seaway (inset). Volcanic rocks, basement uplifts, and Wasatch line are younger than development of thrusting and foreland basin discussed in this paper. AA′ is cross-section line modeled in analysis.

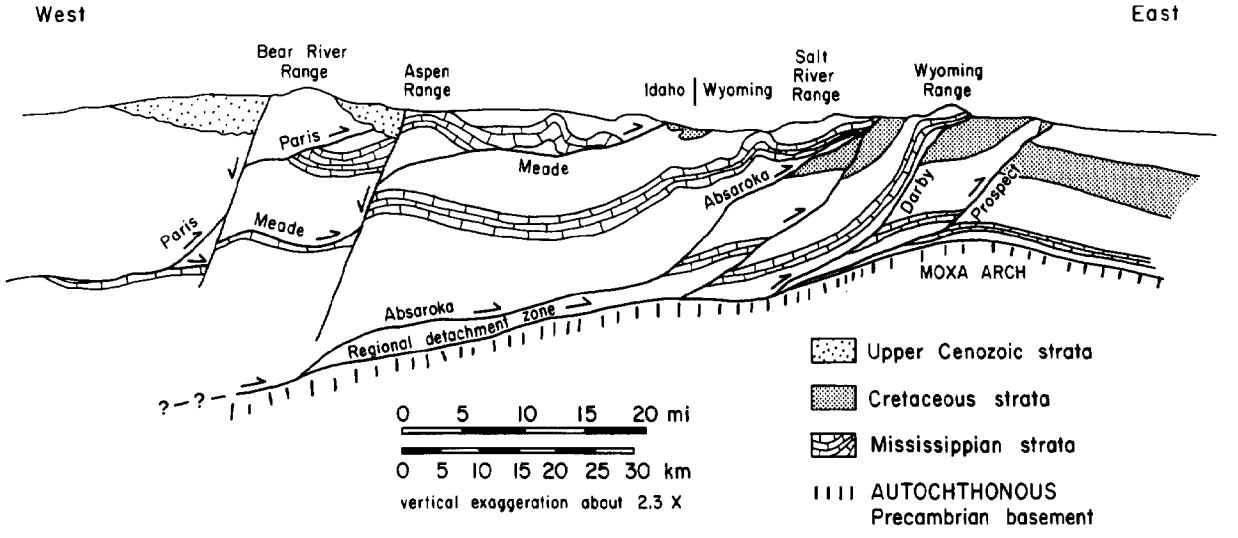

FIG. 2—Generalized schematic cross section across Idaho-Wyoming thrust belt along line AA′ of Figure 1 (after cross section XX′ of Royse et al, 1975), illustrating west-dipping sledrunner form of thrust faults and duplication of section.

Isopach maps of the Upper Cretaceous strata (McGookey et al, 1975) clearly distinguish the subsiding trough adjacent to the thrust belt (Fig. 3). Figure 4 illustrates the stratigraphic framework of the basin adjacent to the Idaho-Wyoming salient of the thrust belt and the ages of the major thrusts. The maximum thicknesses of the various units do not occur at a single location, so Figure 4 is a compilation of the units at their thickest locations. The sum of maximum local thicknesses of beds that accumulated during active deformation in the thrust belt is thus about 9 km.

QUALITATIVE PALINSPASTIC EXAMINATION OF FORELAND BASIN

Knowledge of the original spatial relations between the thrust faults and the depositional basin is essential to an analysis of the relation between the thrust belt and the foreland basin. Because shortening was progressive during the latest Jurassic to early Eocene, it is necessary to make incremental palinspastic reconstructions.

The cross sections (XX′ and YY′) of Royse et al (1975) formed the basis for the palinspastic reconstructions. Shortening was estimated directly from the sections, including both folding and fault offset between hanging-wall and footwall cutoffs of specific horizons. Because offsets on XX′ are larger than on YY′ (Fig. 5), data points north of approximately 42°N were restored slightly farther to the west than were those to the south.

Thicknesses of surface and subsurface sections were then compiled from a variety of maps and other sources. Each data point was restored an appropriate distance in a westerly direction, perpendicular to the local fold axes. Palinspastic isopach maps of six stratigraphic intervals were constructed (Figs. 6-11).

On these palinspastic bases, a simple pattern emerges for the Early Cretaceous: a north-trending axis 100 km wide of maximum accumulation on the west and a broad region of nearly uniform accumulation to the east. The western margins of the Lower Cretaceous isopach maps are largely erosional. Upper Cretaceous patterns are similar, but there is better preservation of the western margins, and secondary maxima in sediment accumulation developed in central Wyoming. The axis of maximum accumulation and eastern hinge line of the trough shifted progressively eastward in Early Cretaceous and early Late Cretaceous times (Fig. 12; Royse et al, 1975, their Fig. 7). The eastward migration is predictable if subsidence was driven by the loading in the thrust belt, which also shifted eastward with time (Armstrong and Oriel, 1965). The reason that the shift ceased in the Coniacian-Santonian interval is not yet clear.

Ages and Continuity of Thrusting

To quantitatively test the proposed relation between thrust belt and foreland basin, the load must be evaluated as a function of time. Armstrong and Cressman (1963), Armstrong and Oriel (1965), and Oriel and Armstrong (1966) first established a chronology for several major thrusts which has been refined, though not significantly changed, by additional data (Fig. 4; Royse et al, 1975; Dorr and Gingerich, 1980).

The precision of dating of individual thrusts is indicated by error bars on Figure 4. In general, most of the uncertainty is due to insufficient preservation of crosscutting and overlapping relations, rather than to doubtful faunal control. For instance, early activity on the Paris thrust is recorded by synorogenic conglomerates in the basal Gannett Group. The clastic strata include latest Jurassic megafossils, which might be redeposited, but Early Cretaceous microfossils in the interbedded lacustrine limestones impose a minimum age on the upper Gannett Group near the Albian-Aptian boundary. Thus, the Paris thrust was active in the latest Jurassic to Early Cretaceous. However, because no prelate Tertiary strata are preserved which overlap the Paris fault trace, the duration of its motion is poorly constrained (Armstrong and Cressman, 1963; Armstrong and Oriel, 1965; Eyer, 1969).

Early Late Cretaceous motion on the Meade thrust is inferred from relations between its probable southern counterpart, the Crawford thrust, and a synorogenic conglomerate, the Echo Canyon Conglomerate (Royse et al, 1975). The transfer of activity from Paris to Meade thrust systems is especially poorly dated. Ex-

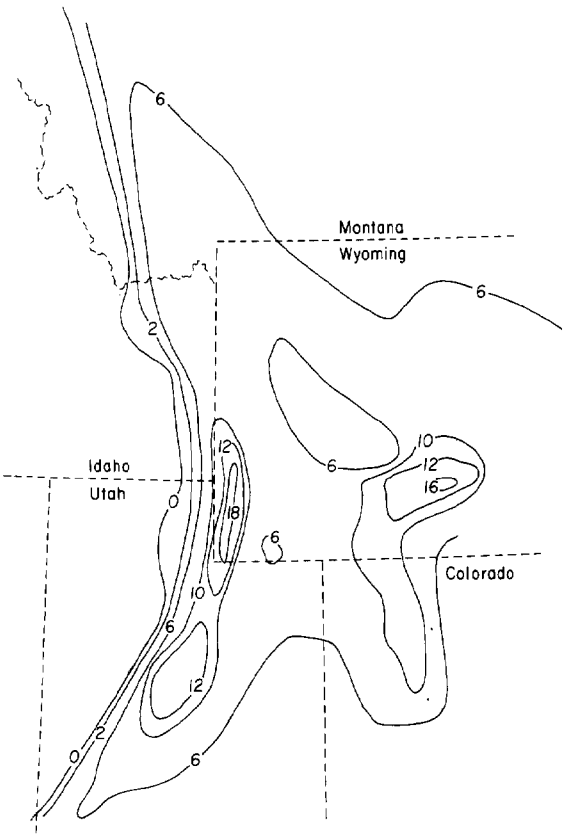

FIG. 3—Restored nonpalinspastic thickness of Upper Cretaceous strata, part of foreland basin of Idaho-Wyoming thrust belt (after McGookey et al, 1975).

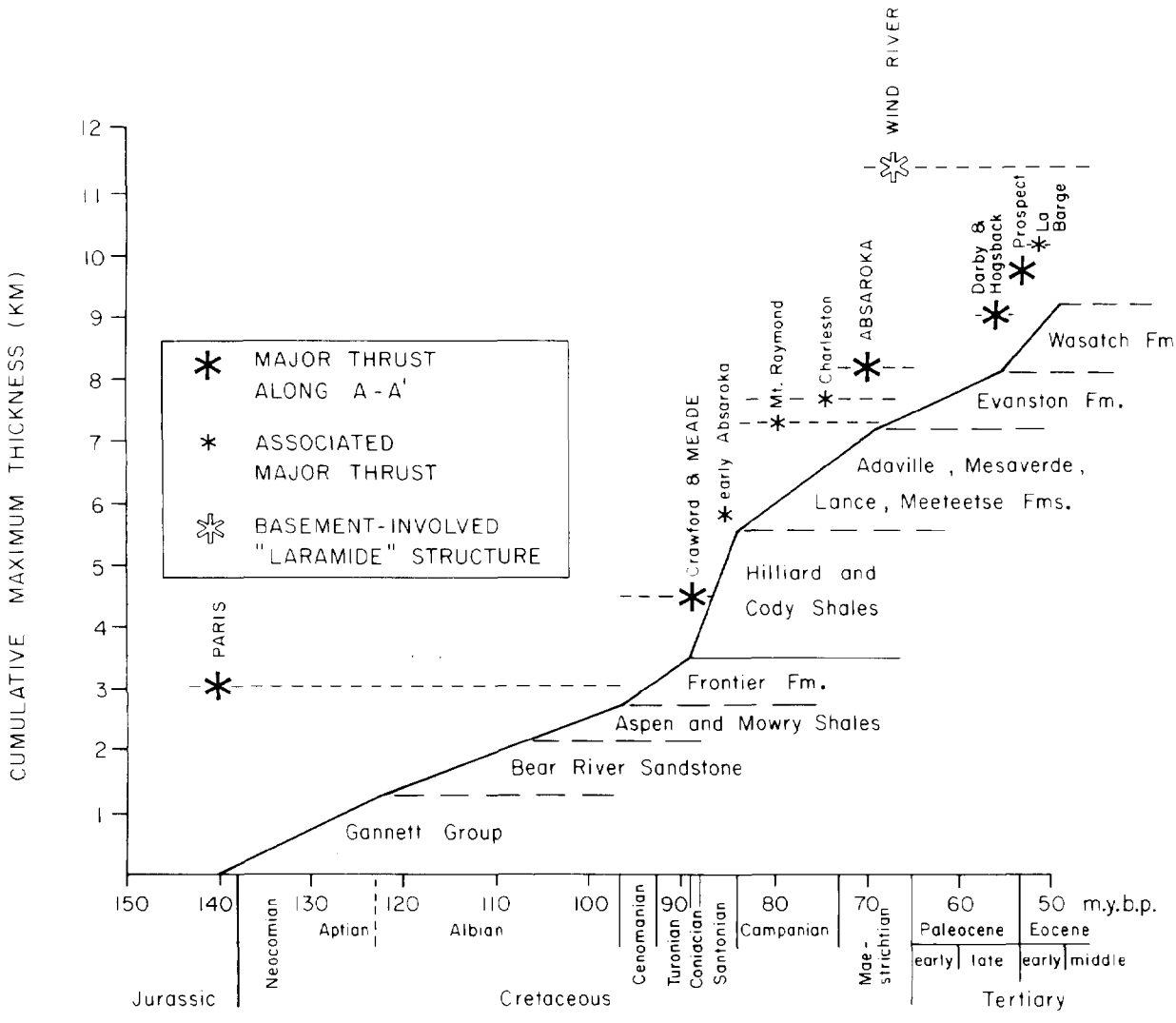

FIG. 4—Stratigraphic framework of Idaho-Wyoming-Utah foreland basin, illustrating maximum thickness of each interval and terminology. Dates on major thrusts in region are noted (large stars = thrusts crossed by line AA', Fig. 1). Dashed lines adjacent to stars indicate age range permitted by these dates (Armstrong and Oriel, 1965; Oriel and Armstrong, 1966; Crittenden, 1974; Royse et al, 1975; Vietti, 1977; and Dorr and Gingerich, 1980). Time scale from Hardenbol and Berggren (1978) and Lanphere and Jones (1978).

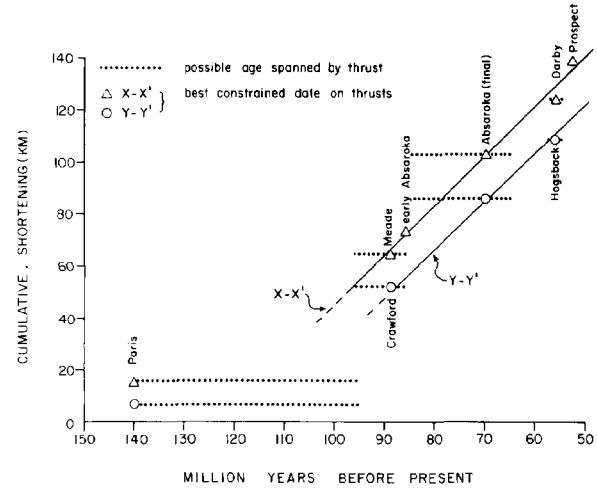

FIG. 5—Cumulative shortening through time on major thrusts in Idaho-Wyoming salient of thrust belt, along two east-west cross sections of Royse et al (1975). XX' corresponds with AA' on Figure 1; YY' is farther south, at about 41°15'N.

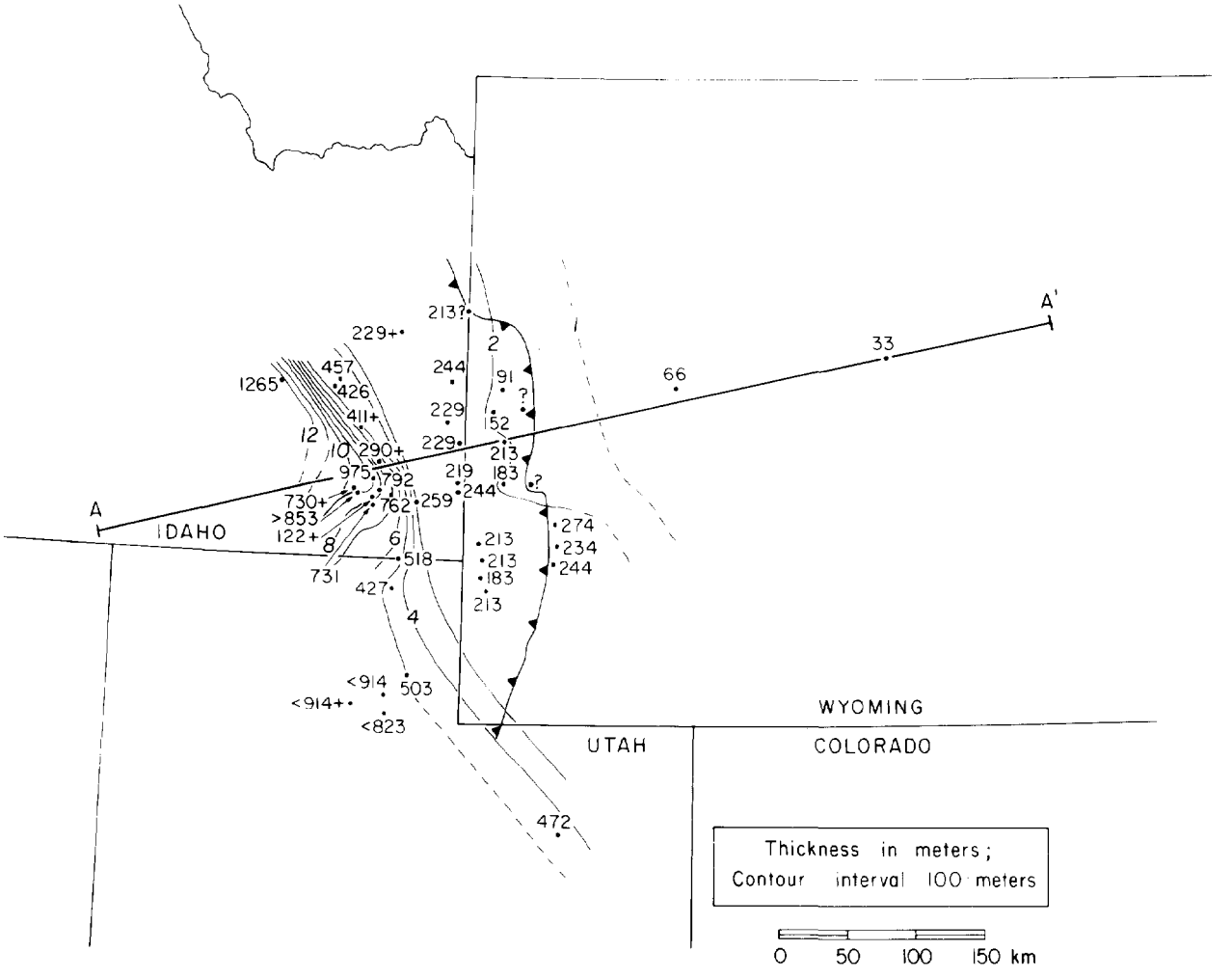

FIG. 6—Palinspastic isopach map of Kimmeridgian(?) to Aptian Gannett Group and correlatives, including basal synorogenic conglomerates which signal initial deformation in thrust belt. Palinspastic restorations based on shortening in Figure 5. Present trace of easternmost exposed thrust (Prospect and Hogsback) indicated with teeth. Thicknesses compiled from Wanless et al (1955), Cressman (1964), Jobin and Schroeder (1964), Eyer (1969), Oriel (1969), Rubey (1973), Rubey et al (1975), Froidevaux (1977), Astin (1977), and Allmendinger (1980).

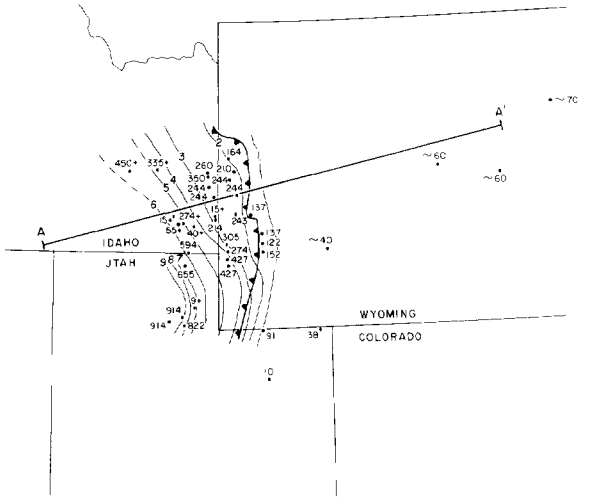

FIG. 7—Palinspastic isopach map of Albian Bear River Sandstone and correlatives, as in Figure 6. Thicknesses compiled from Wanless et al (1955), Jobin and Schroeder (1964), Garvin (1969), Hummell (1969), Oriel (1969), Rubey (1973), Crittenden (1974), McGookey et al (1975), Rubey et al (1975), Maher (1976), Astin (1977), Froidevaux (1977), and Allmendinger (1980).

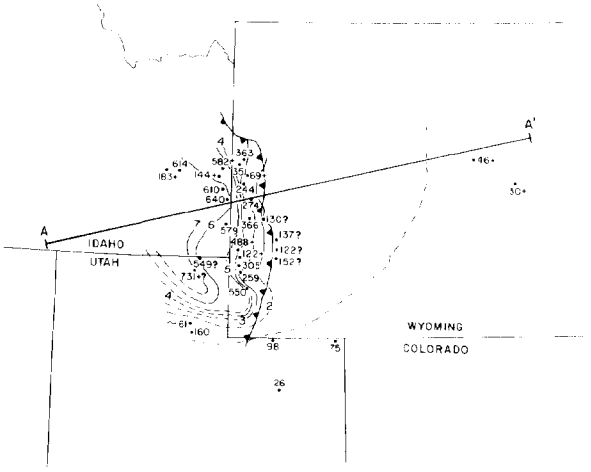

FIG. 8—Palinspastic isopach map of upper Albian Aspen and Mowry Shales and correlatives, as in Figure 6. Thicknesses compiled from Wanless et al (1955), Jobin and Schroeder (1964), Garvin (1969), Hummell (1969), Oriel (1969), Rubey (1973), Crittenden (1974), Rubey et al (1975), Maher (1976), Astin (1977), Froidevaux (1977), Ryer (1977), and Merewether et al (1979).

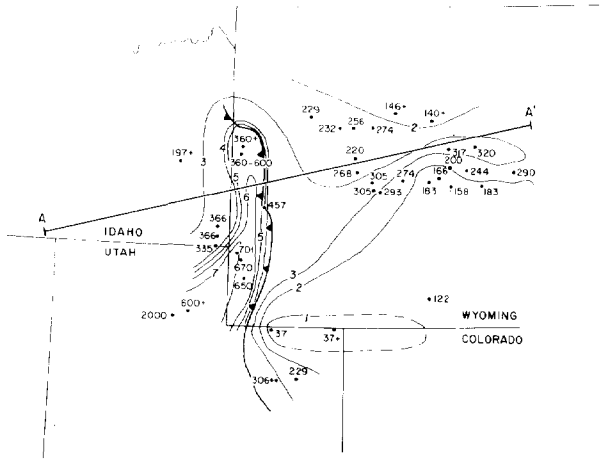

FIG. 9—Palinspastic isopach map of Cenomanian-Turonian Frontier Formation and correlatives (see caption for Figure 6). Thicknesses compiled from Wanless et al (1955), Williams and Madsen (1959), Hale and Van de Graaff (1964), Garvin (1969), Hummell (1969), Oriel (1969), Asquith (1970), Keefer (1972), Rubey (1973), Crittenden (1974), Rubey et al (1975), Astin (1977), Myers (1977), Ryer (1977), and Merewether et al (1979).

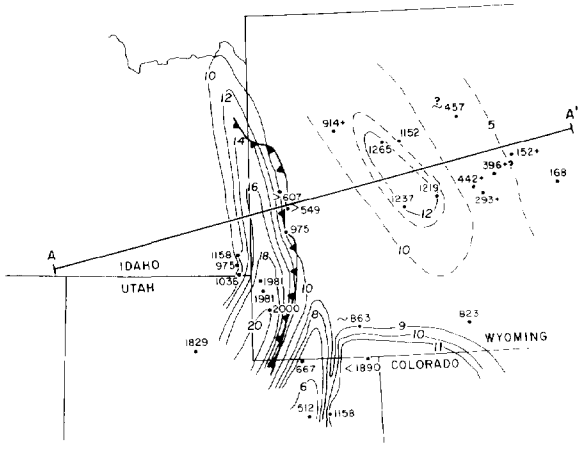

FIG. 10—Palinspastic isopach map of Coniacian-Santonian Hilliard and Cody Shales and correlatives (see caption for Figure 6). Thicknesses compiled from Hale and Van de Graaff (1964), Garvin (1969), Gosar and Hopkins (1969), Hummell (1969), Oriel (1969), Asquith (1970), Keefer (1972), Rubey (1973), Rubey et al (1975), Astin (1977), Ryer (1977), and Merewether et al (1979).

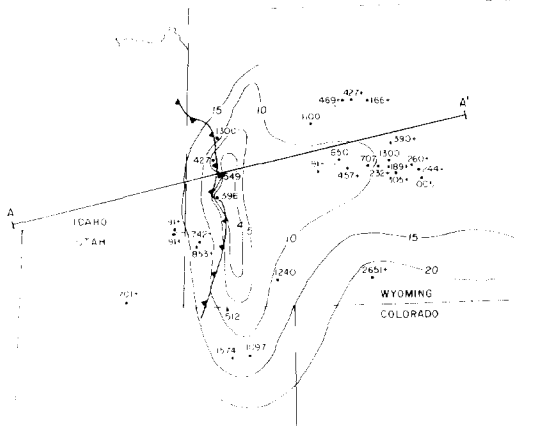

FIG. 11—Palinspastic isopach map of Campanian-Maestrichtian units, including Adaville, Lance, Mesaverde, and Meeteetsee (see Figure 6 for explanation). Thicknesses compiled from Keefer (1960, 1965, 1972), Hale and Van de Graaff (1964), Gill and Cobban (1966), Garvin (1969), Gosar and Hopkins (1969), Oriel (1969), Asquith (1970), Rubey (1973), Rubey et al (1975), Kitely (1976), Astin (1977), and Dorr et al (1977).

posed upper Lower Cretaceous strata are nowhere cut by the Paris thrust, but they are cut by the Meade thrust. However, Schmitt (1980) suggested that conglomerates in the lowest Upper Cretaceous Frontier Formation were derived from the Willard plate, which may correlate with the Paris system (Roberts et al, 1965).

Shortening occurred on the Absaroka thrust system at least twice and is more precisely dated. A synorogenic conglomerate which was almost certainly derived from a hanging-wall anticline in the "early Absaroka thrust" contains identifiable clasts of upper Lower Cretaceous Aspen Shale, whereas shaly interbeds higher in the same unit have mid-Santonian microfossils. Clearly, that unit is post-Early Cretaceous and probably Santonian. Assuming that uplift on the fault was synchronous with deposition of the conglomerate, the fault was active in the Santonian (Royse et al, 1975; Vietti, 1977). That conglomeratic unit was subsequently tightly folded in the hanging wall of the Absaroka thrust, which

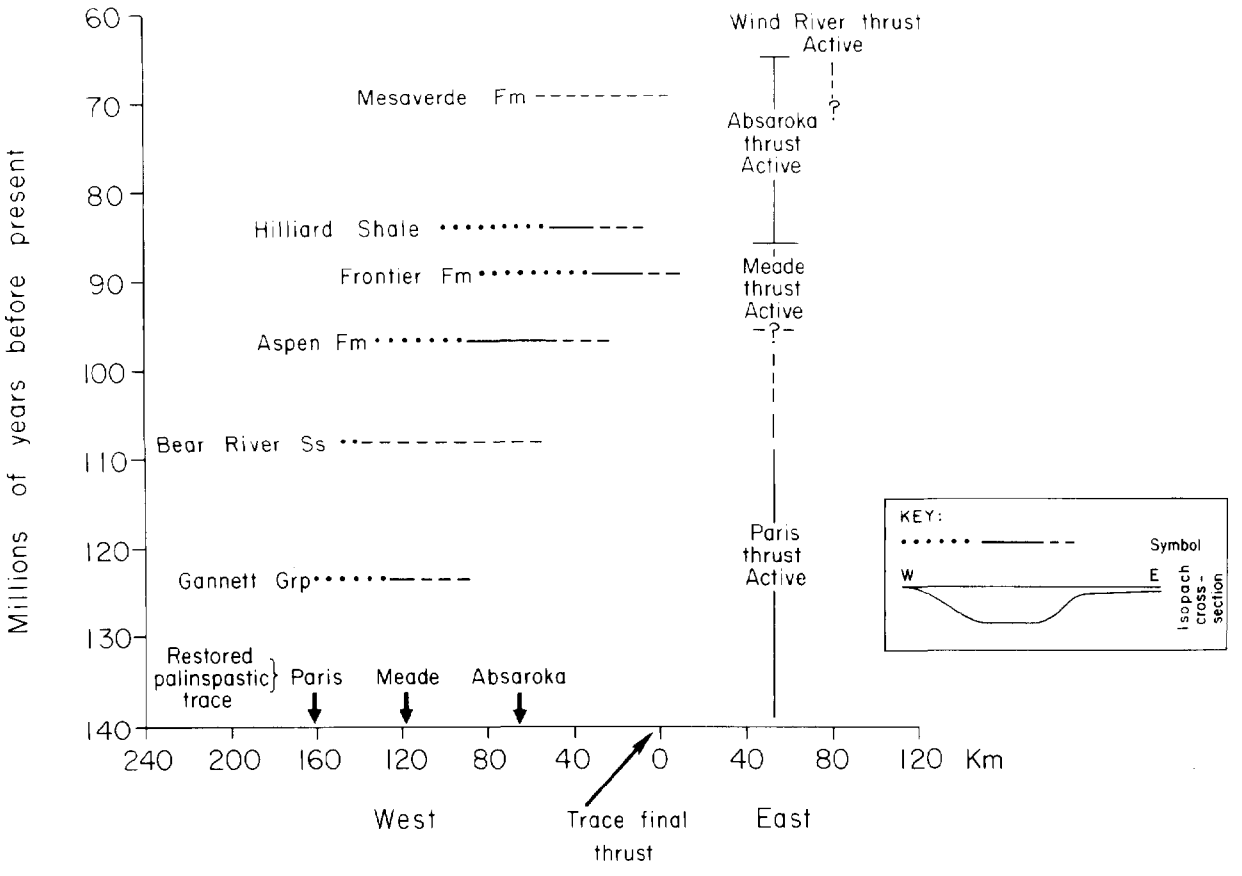

FIG. 12—Graph showing eastward shift of palinspastic position of foreland trough through time.

significantly offsets strata as young as latest Cretaceous and is overlapped by a latest Cretaceous-early Tertiary unit. Thus, primary motion on the Absaroka fault is well constrained as latest Cretaceous (Maestrichtian; Armstrong and Oriel, 1965; Royse et al, 1975). Though post-Maestrichtian faults are more precisely dated (Fig. 4), they are not included in the quantitative model because they clearly overlap in time with the different tectonic, and presumably mechanical, system that created the basement-cored uplifts typified by the Wind River fault.

Realistic quantitative modeling requires proper correlation between loading and the stratigraphic section accumulating in the foredeep at that time. An apparent dilemma arises because deposition in the foreland basin was continuous throughout the Cretaceous, whereas dates on thrusts indicate major discrete pulses of movement. The continuity of thrusting is significant because it determines the continuity of loading. In the quantitative model developed below, resolution of this issue is not vital because the elastic model is linear through time and the three intervals examined are well dated. However, if one were to model the flexural response to loading of a viscoelastic or otherwise nonlinear lithosphere, it would be important to know if thrusting was continuous. Available stratigraphic data in the thrust belt and foreland basin bear on this question, but are not definitive.

In the thrust belt, for example, the Absaroka thrust moved 8 km in the Santonian and about 29 km in the upper Maestrichtian (Royse et al, 1975; Vietti, 1977), indicating shortening in at least two pulses during about 20 million years along a major thrust surface. Also, there is a gap of about 50 million years between the available dates on the Paris and Meade thrusts (Fig. 4), but these dates only limit the time of first motion on the Paris and apparent final motion on the Meade. Shortening could have been continuous throughout that time.

In the foreland basin, the basin axis progressed eastward during the times of motion on the Paris, Meade, and early Absaroka thrusts (Fig. 12) and widespread unconformities are not reported in the marine strata of the foreland basin, although there were major regressive and transgressive cycles (Kauffman, 1977). Both of these observations suggest that loading was continuous through time and that the load shifted eastward, but because erosion and subsequent depositional loading are not uniquely linked to active thrusting, the continuity of events in the basin is not an adequate indicator of continuous thrusting.

These observations do not resolve whether shortening was as episodic as indicated by available dates (Fig. 4), or continuous, or characterized by an intermediate step-function. Clearly much work remains to correlate the patterns of transgression in the basin to specific thrust events in the orogenic belt or to other factors.

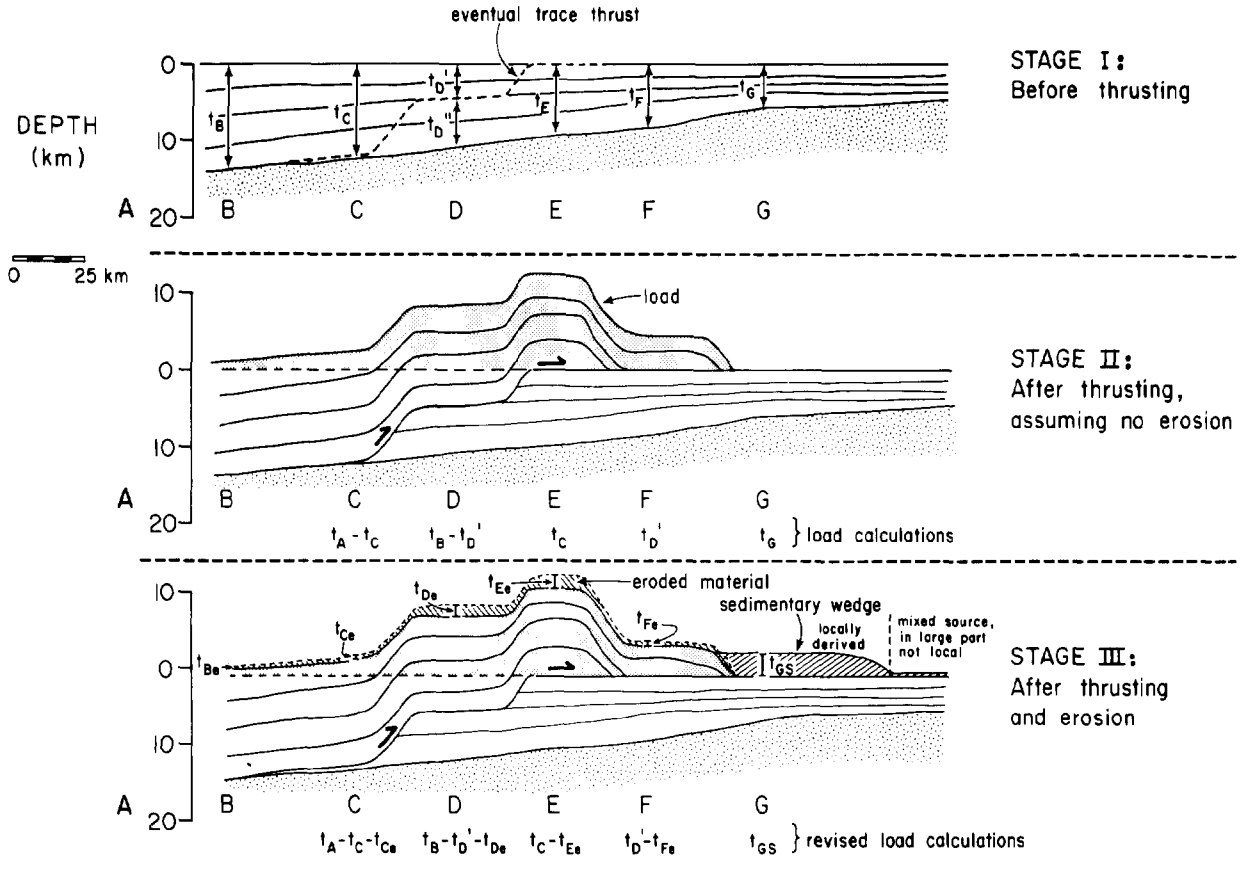

FIG. 13—Method of determining crustal load profiles for each thrust interval. Step I is pre-thrust geometry. During step II, section is duplicated by horizontal shortening. In step III, volume of sediments in thick western part of foreland basin is eroded from thrusts (see text). Loads of both thrusts and basin fill of step III are those used in computations.

QUANTITATIVE MODELING

Correlations

The correlations between thrust sheets and derivative sediments in the foreland trough used in the following analysis are based on available dates and facies relations: (1) the Paris thrust correlates to the Gannett Group, Bear River Sandstone, and Aspen Shale, and their equivalents; (2) the Meade thrust correlates to the Frontier Formation and Hilliard Shale and their coarser clastic equivalents to the west, such as the Echo Canyon conglomerate; and (3) the Absaroka thrust correlates to the Campanian and Maestrichtian strata. The major uncertainty in this correlation is the assignment of the upper Albian strata. Although available dating of thrusts suggests that all the Lower Cretaceous strata equate with the Paris thrust, extrapolation of the linear shortening curve in Figure 5 to include the Early Cretaceous might suggest initiation of the Meade about 110 to 115 m.y., during the Albian.

Estimation of Crustal Loading

Quantitative modeling requires estimation of the amount of crustal loading that occurred during each interval of thrusting. The primary loading is caused by shortening in the upper crust along thrust faults; erosion of the thrust plates and deposition in the basin redistribute that load. The load consists of material that is added above the preexisting topographic surface and is compensated isostatically by flexural subsidence (Fig. 13).

Estimates of crustal loading due to thrusting are derived from cross section XX′ of Royse et al (1975) corresponding with the portion of AA′ of Figure 1 across the thrust belt proper. The cross section was palinspastically reconstructed, matching hanging wall and footwall cutoffs. Then, the change in restored thickness of rock overlying a number of fixed reference points (Fig. 13, locations A, B, C, D, E) was measured as the sections were sequentially shortened along the Paris, Meade, and Absaroka thrusts. A profile of change in load due to each thrust was constructed (Fig. 13, step II, shaded), which was then reduced by an area equal to the cross-sectional area of sedimentary rocks deposited in the western axial part of the foreland basin during the time of shortening (Fig. 13, step III).

The assumption that erosion in the thrust belt is equal

to detritus accumulating in the basin cannot be rigorously proven, but is based on the conceptual model that locally derived debris was deposited immediately adjacent to the mountain front, in the foreland trough. More distantly derived detritus, from extensions of the orogenic belt to the north and south and minor contributions from the east, accumulated to the east along the bathymetric axis of the sea (approximately in central to eastern Wyoming, Kauffman, 1977). The degree of reality in this model linking erosion to a given part of the basin fill probably varies through time. The distribution of erosion over the uplifted surface of the mountain profile is also not known. Bloom (1978) gave an example of the influence of elevation (y) on denudation rate (rate = $y^{(.63)}$). A similar but simpler relation of erosion proportional to elevation to the first power is employed here. The thickness profile of step III (Figs. 13 and 14) times the density of the rock (2.4 gm/cm^3) times the gravitational field strength (g) comprises the change in load above the pre-thrusting ground level.

The load is relatively greater immediately adjacent to ramps in the lower plate, on the side of the ramp toward which the thrust moved (Fig. 13). Thrust faults in a foreland thrust belt characteristically consist of long decollements interrupted by short ramp zones, and ramp zones typically occur near the front limit of thrusting (Fig. 2). Therefore, the load is concentrated in a narrow zone at the edge of the frontal thrust and over the remnants of the frontal parts of older, structurally higher, faults. This causes the irregularity in the load profiles of Figure 14. Smaller and geometrically simpler loads are produced in the back end of a thrust belt, where slightly thicker sections travel toward the craton above a decollement (Fig. 13, step III).

This study ignores probable Cretaceous lateral translation, and thus possibly loading, along westward extensions of the major decollements or other unproved faults in the hinterland, west of the Idaho-Wyoming thrust belt. At present, the structural history and geometry of that region remain poorly known (Oriel and Platt, 1979; Allmendinger and Jordan, 1981). The extent of crystalline basement involvement in thrusting will strongly influence loading. If crystalline involvement was significant, as suggested by Harrison et al (1980) in a comparable structural position in Montana, then ramps will be much more important than if thrusts remain at constant decollement levels in the stratigraphic cover. Options range from a reduction in load in the western area (due to denudation), to no change in load, to a small increase in load. However, because total subsidence at any point is the arithmetic sum of the influence of load elements at varying distances from that point and a load element causes subsidence over a distance of only about 50 to 75 km (Fig. 14), the choice of hinterland structure has little effect on the subsidence of the foreland basin. Hinterland loads are significant in determining the subsidence, and thus elevation, of the thrust belt. The error of neglecting hinterland structure will be largest for the Early Cretaceous model because the data control on load is only about 30 km wide. There, the load thickness drops off to near zero at the west end of the available cross

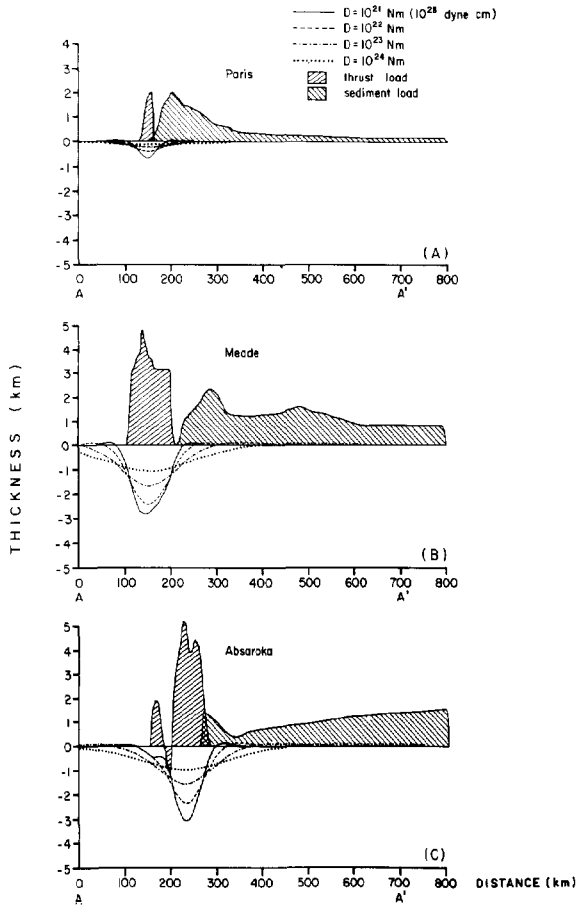

FIG. 14—Comparison of predicted crustal subsidence, due only to 3 thrust loads illustrated, to preserved thickness along AA′ for 4 values of flexural rigidity. Three time intervals are discriminated, corresponding to (A) Paris, (B) Meade, and (C) Absaroka thrusts. Palinspastic thickness of strata also illustrated. Prospect thrust on AA′ (Fig. 1) corresponds to 320 km. Vertical exaggeration 50:1.

section (Fig. 14a), consistent with the interpretation that loading is most important near the frontal end of the thrust.

Similarly, no attempt has been made to incorporate mechanical changes in the lithosphere that occur between the foreland basin and the magmatic arc. Presumably the elastic lithosphere effectively became thinner and softer to the west toward the plutonic belt and thermal conditions rather than structural geometry may have been the primary control on topography. Foreland basin evolution should be relatively insensitive to the thinning of the elastic lithosphere, because loads added on the western part of the lithosphere would have localized isostatic response because of the softer lithospheric properties (Beaumont, 1981).

Loading due to sediment accumulation in the foreland basin and the broader Cretaceous seaway was determined by constructing a cross section along AA′ on each palinspastic isopach map (Figs. 6-11; illustrated in step III, Fig. 13) and summing them for the intervals corresponding to the three loading intervals (Fig. 14).

The cross-sectional area times the present density of the strata (2.4 gm/cm^3) times gravity equals the load in two dimensions.

Although sea level changes play an important role in controlling sedimentation, which then controls loading, the actual weight of the water in a relatively shallow sea has much less effect on lithospheric flexure than does the weight of the strata. Worldwide sea level rise in the Cretaceous (Pitman, 1978; Bond, 1979; Hancock and Kauffman, 1979; Vail and Mitchum, 1979) and local tectonics interacted in the region to produce complexly shifting shoreline positions in the Western Interior seaway (Fig. 15). Overall, however, the region passed from nonmarine conditions at the beginning of the Cretaceous to nonmarine conditions at the end of the Cretaceous (McGookey et al, 1975), for a net change in water load of zero and reached a maximum water depth of perhaps 200 to 300 m (Kaufmann, 1977). Whereas the isostatic response to sea level is not directly computed in this study, its role can be inferred from the topographic profiles that are created (Fig. 15).

Elastic Flexure by Loading

Regional isostatic compensation is the principal driving force of the subsidence in this model, as the lithosphere accommodates the loading by flexure. Lithospheric response is modeled as flexure of a perfectly elastic infinite beam under a distributed load buoyed up by a fluid substratum. Similar analyses have been made for a variety of other sedimentary basins (Watts and Ryan, 1976; Beaumont, 1978, 1979, 1981).

Regional isostatic compensation can be modeled in two ways. The first option is to model flexure due to the uneroded thrust load and assume that the location and degree of erosion in the mountains and sedimentation in the basin are uniquely controlled by the tendency toward isostatic equilibrium. If so, any discrepancy between the theoretical sediment fill and preserved isopachs (Figs. 6-11) indicates subsidence in response to mechanisms other than regional isostatic compensation. The other approach, followed in this study, assumes possible nonequilibrium sediment distribution and computes the flexure due to the thrust load and actual sediment load (Fig. 13). In this example, the test of isostatic compensation as the sole driving force for subsidence is whether or not the predicted final equilibrium topography is geologically realistic.

In this study, finite difference computer modeling has been used, rather than an analytical approach, to make maximum use of the geologic data. The equations and computer model are described in Appendix A.

RESULTS

The subsidence of an elastic lithosphere has been computed for loading by only the thrust plates (Fig. 14) and for total load of the thrusts and basin fill; the latter was used to generate topographic profiles (Fig. 15). Models were generated for four different values of lithospheric flexural rigidity, 10^{21}, 10^{22}, 10^{23}, and 10^{24} Nm (Newton meters) (10^{28}–10^{31} dyne cm). The best-fitting value of flexural rigidity and the general validity of the premise that crustal loading creates the foreland basin can be evaluated.

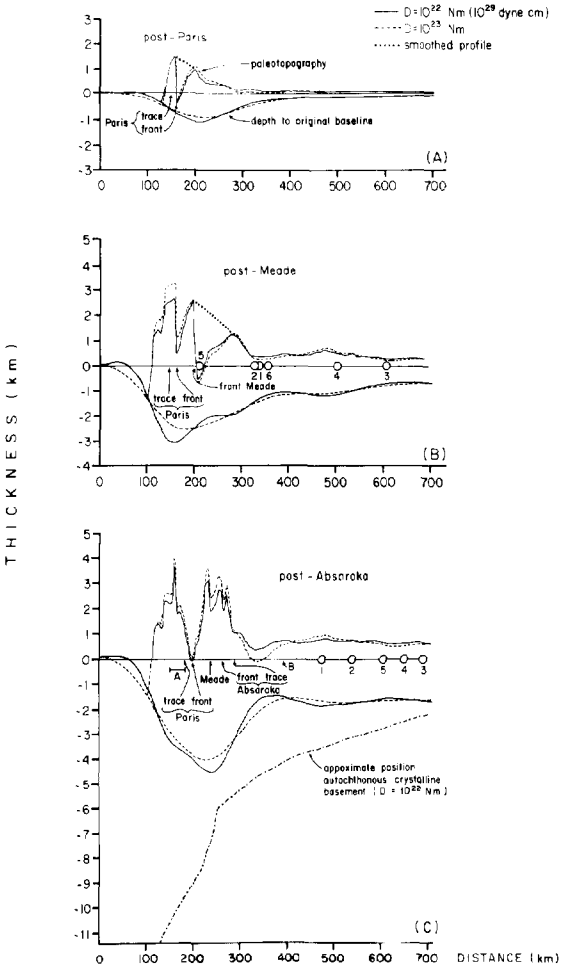

FIG. 15—Predicted topographic profiles and depth to original datum (top autochthonous Jurassic) along AA', following each major thrust event. Prospect thrust occurs at 320 km. Initial base level may have roughly corresponded to sea level in latest Jurassic, but is not shifted here to accommodate sea level changes. Pre-erosion position of major thrusts indicated as "front" and eroded position as "trace." (A) No shorelines shown for Paris (see text). (B) Shoreline designations for Meade (after McGookey et al, 1975): (1) earliest Cenomanian, (2) basal Turonian, (3) upper middle Turonian, (4) basal Coniacian, (5) late Coniacian, and (6) late Santonian. (C) Shorelines for Absaroka: (1) earliest Campanian, (2) early middle Campanian, (3), early late Campanian, (4) late Campanian, (5) early Maestrichtian, and nonmarine by end Maestrichtian. "A" is location of pre-Evanston uplift and "B" is palinspastic position of Wind River thrust (Royse et al, 1975). Vertical exaggeration 50:1.

Crustal loading by only the thrust sheets produces an approximately symmetrical subsidence curve characterized by steep sides and a sharply defined "outer bulge," where a rise in the elastic beam above the zero level is predicted (Fig. 14). Higher values of flexural rigidity, corresponding to a stiffer lithosphere, create profiles with less subsidence and with the outer bulge at a greater distance from the thrust load. Beau-

mont (1981) illustrates the influence of changing flexural rigidity on basin shape. For an Andean-type thrust belt, sediments are not shed toward the heated and strongly uplifted interior of the mountain belt. Although flexure will occur on both sides of the load, a sedimentary basin will form only on the cratonic side.

Comparison of the predicted flexural basin width to the shape of the axis of greatest accumulation immediately adjacent to the thrust belt may indicate the flexural rigidity of the lithosphere, even though the isopachs indicate composite subsidence due to both thrust and sediment loads. For the Meade thrust (Fig. 14b), the predicted subsidence is zero at approximately the eastern margin of the thickest part of the basin fill for a flexural rigidity of 10^{23} Nm. For the Paris load (Fig. 14a), the predicted subsidence has gentle flanks and there is no abrupt eastern limit of the thick basin fill, so it is more difficult to infer a particular value of flexural rigidity, but 10^{22} to 10^{24} Nm are acceptable values. For the Absaroka interval (Fig. 14c), the best fit appears to be 10^{22} Nm, producing an outer bulge or "forebulge" that is located at the actual position of the Maestrichtian Moxa arch, suggested by Elliott (1977) to be a forebulge. However, because of partly coeval Laramide-style deformation (such as the Wind River thrust) and possible ancestral activity, the location of the Moxa arch may not be uniquely controlled by loading and flexure. If it is not a valid forebulge, 10^{23} Nm flexural rigidity is also a reasonable fit.

The load of the basin fill must be included to validly model regional loading and substantially changes the shape of the predicted subsidence curves. For all modeled values of flexural rigidity, the addition of the weight of the strata, more widely distributed than the thrust load, pushes the outer bulge far to the east, beyond the eastern limit of the input data. Thus, a relatively low value of flexural rigidity, or a soft lithosphere, creates a wide sedimentary basin if the total load is distributed over a wide belt.

The predicted final equilibrium topographic profiles for cross section AA′, immediately after each of the three thrust events modeled, are shown in Figure 15 (with 50:1 vertical exaggeration). These were generated by summing (1) total subsidence predicted for the combined thrust plate and basin-fill load, (2) load profiles, and (3) preexisting topography (zero before the Paris, cumulative after each successive thrust). The topographic profiles are not valid west of a point 15 km west of the Paris thrust owing to lack of structural control. Figure 15 also illustrates the depth to which the initial pre-Paris sea level datum (the top of autochthonous Jurassic strata) had subsided after each thrusting, for 10^{22} and 10^{23} Nm flexural rigidity.

From west to east, the topographic profiles of Figure 15 each show (1) a high mountain range overlying the thrust faults; (2) a gently sloping (less than 1.5° eastward-dipping) region of sedimentation, corresponding to alluvial fans and coastal plain; and (3) a flat region on the east corresponding to the ancient sea floor. Given minor limitations and exceptions, this profile is very realistic, conforming satisfactorily to the modern topographic profile on the eastern side of the Andes Mountains, a geologically similar mountain belt (Fig. 16).

Because the predicted topography is reasonable and fits local paleogeographic constraints summarized below, lithospheric loading by thrusting and by subsequent redistribution of the load by sedimentation was apparently the primary cause of subsidence of the seaway flanking the Idaho-Wyoming thrust belt. Other factors, such as sea level change, merely modified an existing downwarp.

DISCUSSION

Assuming that the width of the thick western part of the basin was primarily determined by the thrust plate load, although total width of the basin was strongly modified by the sediment fill load, a flexural rigidity of about 10^{23} Nm (10^{30} dyne cm) is indicated by the basin shape (Fig. 14). This corresponds to an elastic lithosphere about 22 to 48 km thick (for Young's modulus of 10^{12} and 10^{11} dyne cm^{-2}, respectively, and Poisson's ratio of 0.25).

Geophysicists do not yet agree whether the earth's lithosphere behaves elastically or viscoelastically. Good fits of elastic models to topographic profiles of trenches, oceanic islands, and cratonic basins have been found (Haxby et al, 1976; Watts, 1978; Turcotte, 1979). Haxby et al (1976) estimate an elastic thickness of continental lithosphere of 30 to 60 km, varying with thermal changes, comparable with the value estimated in this study. Walcott (1970), Sleep and Snell (1976), and Beaumont (1978; 1981) infer that the lithosphere behaves viscoelastically, based on examination of both continental and oceanic features. However, data are scarce on continental lithospheric flexure over long time spans—only four data points used by Beaumont (1978) seem to represent proper continental lithosphere—and it is difficult to separate variables relevant to the elastic-viscoelastic debate (the age and elastic thickness) from other variables (e.g., thermal history, initial lithospheric thickness, plate motions).

Whereas the best-fitting flexural rigidity can only be approximated for the Paris and Absaroka loads, there is no obvious change in flexural rigidity with time. These results are consistent with elastic behavior of the western North American lithosphere over the modeled 70 million year span.

The accuracy of Cretaceous paleotopographic reconstructions may vary from one thrust model to the next (Fig. 15). The quality of the data constraining the loads and the degree to which regional tectonics fit the simple elastic beam model vary for the three time intervals modeled. Specifically, the thrust load for the Paris interval is more poorly known than for either of the younger faults, because subsurface structure in the western part of the thrust belt is less well known. In addition, there are strong indications that thin-skinned shortening on the Absaroka thrust was partly contemporaneous with the early phase of basement-involved shortening to the east (position of Wind River thrust indicated on Fig. 15; Royse et al, 1975). Uppermost Cretaceous isopach maxima east of the main foreland

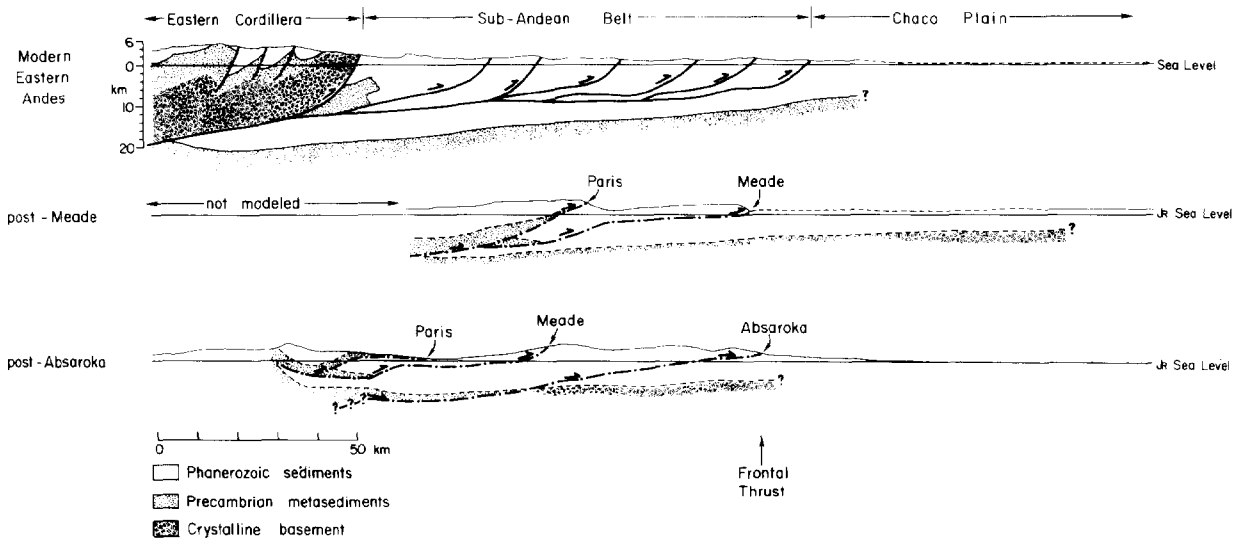

FIG. 16—Comparison of topography of modern Andean foreland thrust belt in northernmost Argentina (from Mingramm et al, 1979) to predicted post-Meade and post-Absaroka topography, showing morphologic segmentation. Meade and Absaroka profiles are shifted laterally to place coeval frontal thrust in line with active frontal thrust in Subandean belt. Andean geology and generalized reconstruction of Cretaceous subsurface geometry show tendency to expose older rocks in more interior part of thrust belt. No vertical exaggeration.

basin axis (Figs. 10 and 11) suggest that subsidence was influenced by factors in addition to the foreland thrust belt (Armstrong and Oriel, 1965; Royse et al, 1975; Cross and Pilger, 1978; Fig. 11). Therefore, the post-Absaroka topographic profile (Fig. 15) is probably in error because it only considers flexural loading due to thin-skinned thrusts, whereas the crust presumably also was being loaded and bent by the Wind River basement-involved thrusting. Thus, the post-Meade topographic profile (Fig. 15) is probably the most accurate, although the eastern part of the post-Paris profile and the western part of the post-Absaroka profile are presumably reliable.

The major apparent problem in the topographic profiles is that a relatively deep "moat" is predicted between the alluvial fans and mountain front. This may easily be dismissed as an artifact of incomplete information. The region immediately adjacent to a given thrust front tends to be the locus of ramps in younger, lower thrusts, creating particularly active uplift and erosion. Consequently, little sediment deposited at the toe of a major thrust is preserved and the toe regions of the thrust faults themselves are poorly preserved (e.g., the present trace of the Paris and Absaroka thrusts are estimated to lie about 11 and 24 km, respectively, west of their original positions; Fig. 15). Although the buried footwalls contain records of the truncated units which initially must have been present in the upper plates as well (therefore the load due to the eroded part of each thrust can be estimated fairly reliably), no similar means exists by which to recover information about the basin fill which was subsequently eroded. Therefore, in the immediate vicinity of the front of each thrust, a realistic thrust load has been input, but sediment fill has certainly been underestimated. In the Paris and Meade profiles (Fig. 15a, b), the moat has been smoothed over by a line showing a more realistic topographic profile. Lacustrine beds in the Gannett Group (Eyer, 1969), a short distance east of the Paris front, suggest that a topographic low may have existed intermittently in this structural position.

Shoreline positions varied complexly in the Cretaceous (McGookey et al, 1975) as shown (numbered from oldest to youngest) on the topographic profiles for the Meade and Absaroka intervals (Fig. 15b, c). They are not shown for Paris time because, after the initial regional nonmarine conditions of the Gannett Group, the Early Cretaceous shorelines were primarily within the belt of eventual thrusting. As McGookey et al (1975, their Figs. 16 and 17) did not use a palinspastic base, their shorelines are not properly located with respect to the profile of Figure 15a. For the Meade and Absaroka intervals, predicted topographic breaks clearly correspond to paleoshoreline positions, particularly where several paleoshorelines cluster together (e.g., 6, 1, 2 of Fig. 15b). In general, the surface slope and local relief both diminish to the east, becoming horizontal east of the easternmost paleoshoreline, implying that the regional depositional base level was the marine basin. At the close of the Absaroka interval, conditions were again nonmarine over the entire length of the profile.

In the east, the height at which the topographic profiles become flat steadily increases through time. This level is 60 m above the initial base line (0 km) after the Paris interval (end of Lower Cretaceous), 250 m after the Meade (end of Santonian), and about 600 m after the Absaroka (end of Cretaceous). This corresponds well to estimates of worldwide sea level rise during this time (Pitman, 1978; Bond, 1979; Hancock and Kauffman, 1979, Vail and Mitchum, 1979). These authors dif-

fer significantly in their estimates of total sea level rise, ranging from 150 to 200 m (Bond, 1979) to 600 m (Hancock and Kauffman, 1979). To a lesser extent they differ in the timing of peak sea level, from about the Coniacian (Pitman, 1978) to the Maestrichtian (Bond, 1979; Hancock and Kauffman, 1979; Vail and Mitchum, 1979). Because the isostatic response to rising sea level is much more complicated than is simple local crustal loading, I have not attempted to model its contribution. Yet, the topographic profiles are consistent with independent evidence that sea level rose throughout the Cretaceous.

Major local relief in the mountain system, constituting individual morphological "ranges" in a modern mountain belt, is predicted (Fig. 15). However, the depth of the valleys may be exaggerated, as they would tend to collect sediments, acting as intramontane basins (Eisbacher et al, 1974). For example, the Canadian Rocky Mountains are subdivided into parallel-trending Foothills, Front Range, Main Range, and Western Range, which are morphologic designations, but all are within the province of the foreland thrust belt. Similarly, the foreland thrust belt of the eastern Andes has two morphologic subdivisions, the Eastern Cordillera on the west and an eastern Subandean Range (Fig. 16). In both regions, each morphologic belt has a slightly different thrusting history, but all contain similar styles of shortening.

In the Idaho-Wyoming thrust belt, the predicted topography has been correlated to the subsurface thrust geometry (Fig. 15). The Absaroka constitutes the most complex example because the older structures have ridden on the Absaroka fault. The ranges in the Absaroka mountain belt clearly correspond to the geometry of the underlying plates; the highest elevations occur above and immediately east of footwall ramps in each stacked thrust. Although Absaroka thrusting produced and/or enhanced uplift over the entire width of the Cretaceous mountain belt, a surface traverse from east to west reveals that each predicted range exposes a progressively older and more deeply eroded thrust system. This is consistent with local geologic constraints. Royse et al (1975) concluded that the central Wasatch Range, along strike of the Bear River and Portneuf Ranges at the west end of Figure 2, was uplifted and eroded between earliest Late Cretaceous and earliest Tertiary time. Those ranges are located on the post-Absaroka topographic profile (Fig. 15c, A), and coincide with a predicted high part of the mountain system, bordered on the east by a deep valley. The erosion function discussed above predicts that about 9 to 10 km of material was eroded from this peak during the Cretaceous, sufficient to expose Cambrian-Ordovician rocks in this part of the upper plate of the Paris thrust. The slight westward dip of the autochthonous crystalline basement (Fig. 15c) is realistic, dipping about 0.5° under the basin and less than 2.5° under the thrust belt.

The Andes of northernmost Argentina and southern Bolivia expose a well-developed young thrust belt with topographic, structural, and age relations much like the Idaho-Wyoming thrust belt in the Cretaceous (Fig. 16). In the low eastern segment, an east-verging foreland thrust belt, the Subandean zone, was not deformed until the late Miocene, but shortening climaxed in the Pliocene and continued into the Pleistocene. The Subandean belt rises to about 2 km above sea level, exposing primarily Mesozoic and Tertiary strata. To the west, significant Miocene deformation, accentuated in the Pliocene, shortened the high eastern Cordillera. There mostly Paleozoic and Precambrian strata are exposed in mountains reaching more than 5 km above sea level (Turner and Mon, 1979; Mingramm et al, 1979). In comparison, predicted paleotopography in the Idaho-Wyoming mountains is about 1.5 to 3.5 km above the coeval sea level.

CONCLUSIONS

Quantitative analysis shows that lithospheric loading due to thin-skinned thrusting, with erosional and depositional redistribution of the load, is adequate to produce a foreland basin many hundreds of kilometers wide. Hence, all additional factors, such as thermal events (Haxby et al, 1976) and sea level fluctuations (Kauffman, 1977), have little influence on subsidence.

The accuracy of predicted topography is limited by probable inaccuracies of the load estimates and regional tectonic interactions. The Paris thrust load is more poorly known than younger loads and uncertainties about the Paris thrust geometry carry forward in time just as the Paris fault was carried eastward as part of the load in the younger, structurally lower Meade and Absaroka thrusts. Shortening on the Wind River thrust influenced subsidence in the uppermost Cretaceous. The end of the eastward migration of the eastern margin of the foreland trough after the Coniacian (Fig. 12) suggests that Santonian subsidence east of the Moxa arch was already influenced by other tectonic systems. It is possible that the final eastward position of the thick foreland basin axis was predetermined by an ancestral or Cretaceous inhomogeneity across which the lithosphere did not flex as an idealized infinite elastic beam. If so, the eventual easternmost position of thin-skinned thrusting (the Prospect-LaBarge system) was predetermined either by the same inhomogeneity or by the final position of its foreland basin. However, that inhomogeneity was not the Paleozoic miogeoclinal hinge line, because its palinspastic position lay to the west, near the Wasatch line.

Thus, the primary cause of the Cretaceous seaway was the development of an extensive, elongate foreland thrust belt in the North American Cordillera. Although Cretaceous sea level rises might have caused widespread flooding of the craton in the absence of an orogenic belt, the subsidence and sedimentation that characterized the seaway were shaped by lithospheric loading in the thrust belt and then by loading with the eroded sediments filling the foreland trough. Had sea level remained fixed or fallen, a thick, wide clastic sediment wedge would still have formed. The role of loading in determining the complex pattern of transgressions and regressions superimposed on the long-term flooding has not been directly investigated in this study, but is probably of primary significance.

APPENDIX A

The subsidence due to thrust and sediment loading was determined by two-dimensional finite difference modeling. Hetenyi (1974) derived the equation describing subsidence of a point j a distance x from the origin, on an infinite elastic beam buoyed by a fluid substratum, due to load i of magnitude h and width 2a. If that point load is centered at a distance s away from the origin, the deflection w of point j will be

$$(1) \qquad w_j = \frac{h_i \lambda}{2K} (\exp(-\lambda a))(\cos \lambda a + \sin \lambda a).$$

The term λ includes both the buoyancy of the mantle beneath the crust (the fluid substratum) and the flexural rigidity of the lithosphere; K is the hydrostatic restoring force, $(\varrho_m$ and $\varrho_a)g$. For selected values of flexural rigidity, D,

$$(2) \qquad \lambda = \left(\frac{(\varrho_m - \varrho_a)\, g}{4D} \right)^{1/4}$$

where ϱ_m and ϱ_a are density of mantle (3.4 gm/cm^3) and air (.00129 gm/cm^3), respectively, and g is 981 cm/sec^2.

Integration of equation (1) over both an entire load, composed of a set of point load elements I, and over all subsiding points J, yielded the three equations with which the data were actually analyzed. Where j was left of i, subsidence w_{ij} was computed as

(3)

$$w_{ij} = \frac{-h}{2} \frac{(\varrho_s - \varrho_a)}{(\varrho_m - \varrho_a)} \left[\exp((-\lambda)(-x + s - a))\cos((\lambda)(-x + s - a)) - \exp((-\lambda)(-x + s + a))\cos((\lambda)(-x + s + a)) \right]$$

where ϱ_s is the density of the strata (2.4 gm/cm^3).

If j was below i,

(4)

$$w_{ij} = -\frac{h}{2} \frac{(\varrho_s - \varrho_a)}{(\varrho_m - \varrho_a)} \left[2 - \exp((-\lambda)(x - s + a))\cos((\lambda)(x - s + a)) - \exp((-\lambda)(-x + s + a))\cos((\lambda)(-x + s + a)) \right] .$$

If j lay to the right of i,

(5)

$$w_{ij} = +\frac{h}{2} \frac{(\varrho_s - \varrho_a)}{(\varrho_m - \varrho_a)} \left[\exp((-\lambda)(x - s + a))\cos((\lambda)(x - s + a)) - \exp((-\lambda)(x - s - a))\cos((\lambda)(x - s - a)) \right]$$

A data set describing each load profile was input on punch cards, consisting of the location s of each element 5.5 km wide, and height h of that load element. For this study, there were three data sets for thrust loads and six for stratigraphic loads.

For a selected input value of flexural rigidity, D, λ was computed. Each load profile containing I load elements was treated individually. To compute the subsidence of each 5.5-km-wide response element I to J on a cross section due to a load element h_i, the position of an element j relative to the load element i was determined, and subsidence w_{ij} found from the appropriate equation (2), (3), or (4). This w_{ij} was added to the subsidence at j due to all preceding load elements. The subsidence w_{ij} was then computed for the j + 1 response element.

After all J elements were analyzed for load element i, the i + 1 load element was input and subsidence w_i caused by it determined, until all I load elements were considered.

The combined subsidence w_{ij} due to each of the nine data sets was stored, and output both on a line printer and a calcomp plotter. The total subsidence in three time intervals, corresponding to a thrust plate and strata filling the basin while that thrust was active, was summed, stored, and plotted. To determine the predicted topography, the total subsidence in each time interval was then added to the input load profile for that time interval.

This sequence was repeated for incremental values of the flexural rigidity, D.

REFERENCES CITED

Allmendinger, R. W., 1980, Geologic map of the southern half of the Ammon 15′ quadrangle, Bingham and Bonneville Counties, Idaho: U.S. Geol. Survey Misc. Field Studies 1259.

_____ and T. E. Jordan, 1981, Mesozoic evolution, hinterland of the Sevier orogenic belt: Geology, v. 9, p. 308-313.

Armstrong, F. C., and E. R. Cressman, 1963, The Bannock thrust zone, southeastern Idaho: U.S. Geol. Survey Prof. Paper 374-J, 22 p.

_____ and S. S. Oriel, 1965, Tectonic development of the Idaho-Wyoming thrust belt: AAPG Bull., v. 49, p. 1847-1866.

Asquith, G. O., 1970, Depositional topography and major marine environments, Late Cretaceous, Wyoming: AAPG Bull., v. 54, p. 1184-1224.

Astin, G. K., 1977, Geology and hydrocarbon potential of Co-op Creek quadrangle, Wasatch County, Utah: Wyoming Geol. Assoc. Guidebook, 29th Ann. Field Conf., p. 543-548.

Beaumont, C., 1978, The evolution of sedimentary basins on a visco-elastic lithosphere: theory and examples: Royal Astron. Soc. Geophys. Jour., v. 55, p. 471-497.

_____ 1979, Foreland basins (abs.): Internat. Union Geodesy and Geophysics, Gen. Assem., Abs., No. 17, p. 3/9.

_____ 1981, Foreland basins: Royal Astron. Soc. Geophys. Jour., v. 65, p. 291-329.

Bloom, A. L., 1978, Geomorphology: Englewood Cliffs, N.J., Prentice Hall, Inc., 510 p.

Bond, G. C., 1979, Evidence for some uplifts of large magnitude in continental platforms, *in* T. R. McGetchin and R. B. Merrill, eds., Plateau uplift: mode and mechanism: Tectonophysics, v. 61, p. 285-305.

Bott, M. H. P., 1979, Subsidence mechanisms at passive continental margins, *in* Geological and geophysical investigations of continental margins: AAPG Mem. 29, p. 3-10.

Cressman, E. R., 1964, Geology of the Georgetown Canyon-Snowdrift Mountain area, southeastern Idaho: U.S. Geol. Survey Bull. 1153, 105 p.

Crittenden, M. D., Jr., 1974, Regional extent and age of thrusts near Rockport Reservoir and relation to possible exploration targets in northern Utah: AAPG Bull., v. 58, p. 2428-2435.

Cross, T. A., and R. H. Pilger, Jr., 1978, Tectonic controls of Late Cretaceous sedimentation, western interior, USA: Nature, v. 274, p. 653-657.

Dickinson, W. R., 1974, Plate tectonics and sedimentation, *in* Tectonics and sedimentation: SEPM Spec. Pub. 22, p. 1-27.

Dorr, J. A., Jr., and P. D. Gingerich, 1980, Early Cenozoic mammalian paleontology, geologic structure, and tectonic history in the overthrust belt near La Barge, western Wyoming: Wyoming Univ. Contr. Geology, v. 18, no. 2, p. 101-115.

_____ D. R. Spearing, and J. R. Steidtmann, 1977, The tectonic and synorogenic depositional history of the Hoback basin and adjacent areas: Wyoming Geol. Assoc. Guidebook 29th Ann. Field Conf., p. 549-562.

Eisbacher, G. H., M. A. Carrigy, and R. B. Campbell, 1974, Paleodrainage pattern and late-orogenic basins of the Canadian Cordillera, *in* Tectonics and sedimentation: SEPM Spec. Pub. 22, p. 143-166.

Elliott, D., 1977, Structural and stratigraphic consequences for the foreland of tectonic activity in the thrust belt (abs.): Joint Wyoming-Montana-Utah Geol. Assoc.

Eyer, J. A., 1969, Gannett Group of western Wyoming and southeastern Idaho: AAPG Bull., v. 53, p. 1368-1390.

Froidevaux, C. M., 1977, Geology of the Hoback area in the overthrust belt, Lincoln and Sublette Counties, Wyoming: Wyoming Geol. Assoc. Guidebook, 29th Ann. Field Conf., p. 563-584.

Garvin, R. F., 1969, Bridger Lake field, Summit County, Utah: Intermountain Assoc. Geologists, 16th Ann. Field Conf. Guidebook, p. 109-115.

Gill, J. R., and W. A. Cobban, 1966, The Red Bird section of the Upper Cretaceous Pierre Shale in Wyoming: U.S. Geol. Survey Prof. Paper 393-A, 73 p.

Gosar, A. J., and J. C. Hopkins, 1969, Structure and stratigraphy of the southwest portion of the Rock Springs uplift, Sweetwater County, Wyoming: Intermountain Assoc. Geologists, 16th Ann.

Field Conf. Guidebook, p. 87-90.
Hale, L. A., and F. R. Van de Graaff, 1964, Cretaceous stratigraphy and facies patterns–northeastern Utah and adjacent areas: Intermountain Assoc. Petrol. Geologists, 13th Ann. Field Conf. Guidebook, p. 115-138.
Hancock, J. M., and E. G. Kauffman, 1979, The great transgressions of the Late Cretaceous: Geol. Soc. London Jour., v. 136, p. 175-186.
Hardenbol, J., and W. A. Berggren, 1978, A new Paleogene numerical time scale, *in* The geologic time scale: AAPG Studies in Geology 6, p. 213-234.
Harrison, J. E., M. D. Kleinkopf, and J. D. Wells, 1980, Phanerozoic thrusting in Proterozoic Belt rocks, northwestern United States: Geology, v. 8, p. 407-411.
Haxby, W. F., D. L. Turcotte, and J. M. Bird, 1976, Thermal and mechanical evolution of the Michigan basin: Tectonophysics, v. 36, p. 57-75.
Hetenyi, M., 1974, Beams on elastic foundation: Univ. Michigan Press, 255 p.
Hummell, S. M., 1969, Anatomy of a gas field—Clay basin, Daggett County, Utah: Intermountain Assoc. Geologists, 16th Ann. Field Conf. Guidebook, p. 117-126.
Jobin, D. A., and M. L. Schroeder, 1964, Geology of the Irwin quadrangle, Bonneville County, Idaho: U.S. Geol. Survey Mineral Inv. Field Studies Map MF-287.
Kauffman, E. G., 1977, Geological and biological overview: western interior Cretaceous basin: The Mountain Geologist, v. 14, nos. 3-4, p. 75-99.
Keefer, W. R., 1960, Progressive growth of anticlines during Late Cretaceous and Paleocene time in central Wyoming: U.S. Geol. Survey Prof. Paper 400-B, p. 233-236.
_____ 1965, Stratigraphy and geologic history of the uppermost Cretaceous, Paleocene and lower Eocene rocks in the Wind River Basin, Wyoming: U.S. Geol. Survey Prof. Paper 495-A, 77 p.
_____ 1972, Frontier, Cody, and Mesaverde formations in the Wind River and southern Bighorn Basins, Wyoming: U.S. Geol. Survey Prof. Paper 495-E, 23 p.
Kitely, L. W., 1976, Marine shales and sandstones in the Upper Cretaceous Pierre Shale at the Francis Range, Laramie County, Wyoming: The Mountain Geologist, v. 13, no. 1, p. 1-19.
Lanphere, M. A., and D. L. Jones, 1978, Cretaceous time scale from North America, *in* The geologic time scale: AAPG Studies Geology 6, p. 259-268.
Lorenz, J., 1980, Lithospheric flexure and the history of the Sweetgrass arch, northwestern Montana (abs.): Geol. Soc. America Abs. with Programs, v. 12, p. 473.
Maher, P. D., 1976, The geology of the Pineview field area, Summit County, Utah, *in* Symposium on geology of Cordilleran hingeline: Rocky Mountain Assoc. Geologists, p. 345-350.
McGookey, D. P., et al, 1975, Cretaceous system, *in* Geologic atlas of the Rocky Mountain Region, United States of America: Rocky Mountain Assoc. Geologists, p. 190-228.
Merewether, E. A., W. A. Cobban, and E. T. Cavanaugh, 1979, Frontier Formation and equivalent rocks in eastern Wyoming: The Mountain Geologist, v. 16, no. 3, p. 67-102.
Mingramm, A., et al, 1979, Sierra Subandinas: Cordoba, Argentina, Second Symposium on Geologia Regional Argentina, p. 95-137.
Myers, R. C., 1977, Stratigraphy of the Frontier Formation (Upper Cretaceous), Kemmerer area, Lincoln County, Wyoming: Wyoming Geol. Assoc. Guidebook, 29th Ann. Field Conf., p. 271-311.
Oriel, S. S., 1969, Geology of the Fort Hill quadrangle, Lincoln County, Wyoming: U.S. Geol. Survey Prof. Paper 594-M, 40 p.
_____ and F. C. Armstrong, 1966, Times of thrusting in Idaho-Wyoming thrust belts: reply: AAPG Bull., v. 50, p. 2614-2621.
_____ and L. B. Platt, 1979, Younger-over-older thrust plates in southeastern Idaho (abs.): Geol. Soc. America Abs. with Programs, v. 11, p. 298.
Pitman, W. C., III, 1978, Relationship between eustacy and stratigraphic sequences of passive margins: Geol. Soc. America Bull., v. 89, p. 1320-1403.
Price, R. A., 1973, Large-scale gravitational flow of supracrustal rocks, southern Canadian Rockies, *in* K. A. DeJong and R. Scholten, eds., Gravity and tectonics: New York, Interscience, John Wiley and Sons, p. 491-502.
Roberts, R. J., et al, 1965, Pennsylvanian and Permian basins in northwestern Utah, northeastern Nevada, and south-central Idaho: AAPG Bull., v. 49, p. 1926-1956.
Royse, F., Jr., M. A. Warner, and D. L. Reese, 1975, Thrust belt structural geometry and related stratigraphic problems, Wyoming-Idaho-northern Utah: Rocky Mountain Assoc. Geologists, 1975, Guidebook, p. 41-54.
Rubey, W. W., 1973, Geologic map of the Afton quadrangle and part of the Big Piney quadrangle, Lincoln and Sublette Counties, Wyoming: U.S. Geol. Survey Misc. Geol. Inv. Map I-686.
_____ S. S. Oriel, and J. I. Tracey, Jr., 1975, Geology of the Sage and Kemmerer 15-minute quadrangle, Lincoln County, Wyoming: U.S. Geol. Survey Prof. Paper 855, 18 p.
Ryer, T. A., 1977, Patterns of Cretaceous shallow-marine sedimentation, Coalville and Rockport area, Utah: Geol. Soc. America Bull., v. 88, p. 177-188.
Schmitt, J., 1980, Depositional environment and tectonic implications of the Coalville conglomerate member, Cretaceous Frontier Formation, Coalville, Utah (abs.): Geol. Soc. America Abs. with Programs, v. 12, no. 6, p. 303.
Sleep, N. H., and N. S. Snell, 1976, Thermal contraction and flexure of mid-continent and Atlantic marginal basins: Royal Astron. Soc. Geophys. Jour., v. 45, p. 125-154.
Speed, R. C., and N. H. Sleep, 1980, Antler orogeny: a model (abs.): Geol. Soc. America Abs. with Programs, v. 12, p. 527.
Steckler, M. S., and A. B. Watts, 1978, Subsidence of the Atlantic-type continental margin off New York: Earth and Planetary Sci. Letters, v. 41, p. 1-13.
Turcotte, D. L., 1979, Flexure: Advances in geophysics, v. 21, p. 51-86.
Turner, J. C. M., and R. Mon, 1979, Cordillera Oriental: Cordoba, Argentina, Second Symposium on Geologia Regional Argentina, p. 57-94.
Vail, P. R., and R. M. Mitchum, Jr., 1979, Global cycles of relative changes of sea level from seismic stratigraphy, *in* Geological and geophysical investigations of continental margins: AAPG Mem. 29, p. 469-472.
Vietti, J. S., 1977, Structural geology of the Ryckman Creek anticline area, Lincoln and Uinta Counties, Wyoming: Wyoming Geol. Assoc. Guidebook, 29th Ann. Field Conf., p. 517-522.
Walcott, R. I., 1970, Flexural rigidity, thickness, and viscosity of the lithosphere: Jour. Geophys. Research, v. 75, p. 3941-3954.
Wanless, H. R., R. L. Belknap, and H. Foster, 1955, Paleozoic and Mesozoic of Gros Ventre, Teton, Hoback, and Snake River Ranges, Wyoming: Geol. Soc. America Mem. 63, 90 p.
Watts, A. B., 1978, An analysis of isostasy in the world's oceans—1. Hawaiian Emperor seamount chain: Jour. Geophys. Research, v. 83, p. 5989-6004.
_____ and W. B. F. Ryan, 1976, Flexure of the lithosphere and continental margin basins: Tectonophysics, v. 36, p. 25-44.
Williams, N. C., and J. H. Madsen, Jr., 1959, Late Cretaceous stratigraphy of the Coalville area, Utah: Intermountain Assoc. Geologists 10th Ann. Field Conf., p. 122-125.